Emission Tomography of Flame Radicals

Hertz, H. M; Faris, G. W

Published in:
Optics Letters

DOI:
10.1364/OL.13.000351

1988

Emission tomography of flame radicals

H. M. Hertz and G. W. Faris

Department of Physics, Lund Institute of Technology, P.O. Box 118, S-22100 Lund, Sweden

Received December 31, 1987; accepted February 25, 1988

We describe a simple experimental arrangement for emission tomographic measurements of radicals in flames. Experimental determinations of two-dimensional spatially resolved distributions of excited-state CH in atmospheric-pressure flames are presented. Calibration of the distributions to absolute number densities is performed with a Rayleigh scattering technique. Methods for simultaneous recording of two to six emission projections and reconstruction from very few (two or three) projections are experimentally investigated. The potential of emission tomography with high temporal resolution for monitoring, e.g., explosions or turbulent flames, is discussed.

Spatially resolved measurements of combustion parameters are of great importance in combustion studies.[1] However, many classical methods used in combustion research are integrating (e.g., emission, absorption, and interferometry). By using tomographic techniques, two- or three-dimensional distributions of a parameter can be reconstructed from multiangular integrated measurements of that parameter. In this Letter an emission tomographic method for two-dimensional spatially resolved measurements of excited flame radicals is presented.

Computer-assisted tomography is well established for x-ray imaging in medicine and has applications in many other fields.[2] By using optical radiation, tomography permits the measurements of temperature,[3,4] refractive index,[5] and species concentration.[6] Tomography based on emission measurements has applications in medicine (e.g., positron-emission tomography[7]) and for microwave imaging of the Sun.[8] Optical emission tomography has been used in plasma studies[9] and for temperature determination in flames from measurements of IR emission.[10]

We have performed tomographic reconstruction of excited-state CH radicals (CH*) in flames from measurements of their emission. Owing to the strong temperature dependence of the reaction mechanisms involved in the production of CH*,[11] this radical is an excellent flame-front indicator (see, e.g., Ref. 12). This makes it suitable for monitoring the development of explosions or turbulent combustion. Furthermore, we describe a method to calibrate the reconstructed distributions to excited-state CH number density that may prove useful for improving models of CH flame chemistry. Such quantitative measurements do not require the tunable-laser source necessary for optical absorption tomography measurements, which yield the ground-state number density.

Since many flames exhibit a fast time dependence, simultaneous recording of the multiangular projections for optical tomography is desirable. Much of the previous flame tomography work[3-6,10] examined steady-state flames by using sequentially recorded projections. Exceptions of this are a 10-kHz laser-absorption system for six projection angles[13] and two complex holographic arrangements for the simultaneous recording of 16–36 interferograms.[14] However, in Ref. 14 the projections were not recorded electronically, making further data processing inconvenient. Since electronic detection requires expensive equipment we have developed a simple technique to multiplex two to three emission projections on a single diode array.

A steady-state flame may be examined with sequential recording of the projections by rotating the flame. Figure 1(a) shows the experimental arrangement. The flame is imaged with a 300-mm focal-length lens on a horizontal intensified diode array (EG&G Model OMAIII) through an aperture and an interference filter. The 436-nm (50-nm FWHM) interference filter is angle tuned to the 431-nm $A\,^2\Delta$–$X\,^2\Pi$ CH transition. The contribution of the weak (2, 0) $A\,^3\Pi$–$X\,^3\Pi$ C_2 transition around 438 nm is negligible for most flame types. Furthermore, C_2* is also restricted to the flame-front region. The long distance between the flame and the lens (1000 mm) in combination with moderate aperture diameters permits the use of a parallel-beam geometry for the tomographic reconstruction. The diameter of the aperture determines the depth of focus and thus the lateral resolution. Thus

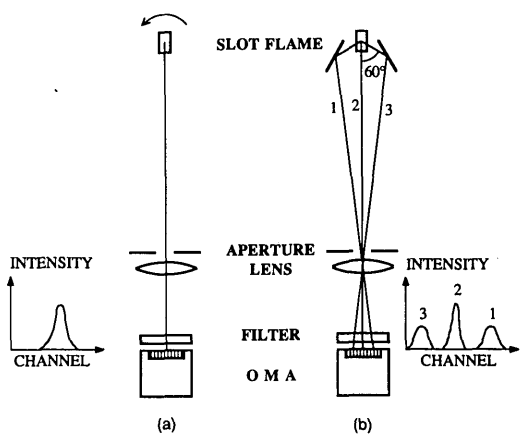

Fig. 1. Experimental arrangement for (a) sequential recording of projections and (b) simultaneous recording of three projections with an optical multichannel analyzer (OMA).

0146-9592/88/050351-03$2.00/0

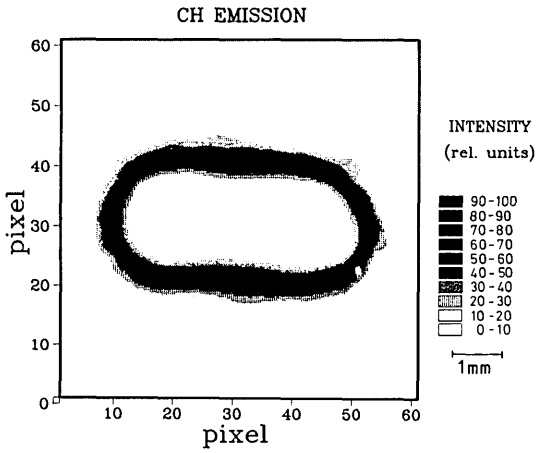

Fig. 2. Tomographic reconstruction of the CH emission of a premixed methane–oxygen flame near the burner. Each pixel is 120 μm × 120 μm. Eight sequentially recorded projections were used.

the aperture is adjusted for maximum resolution while a sufficient signal-to-noise ratio is still maintained in the projections for reliable tomographic reconstruction. Normally the resolution is determined by geometrical optics, but for small apertures diffraction effects become significant.[15] The lateral resolution was measured experimentally by imaging a vertical glowing 25-μm platinum wire on the diode array.[16] The vertical resolution is determined by a slit in front of the diode array.

Figure 2 shows a 61 × 61 pixel tomographic reconstruction of the CH emission from a lean premixed atmospheric methane–oxygen 2.5 mm × 5 mm slot flame. The tomographic reconstruction algorithm is described below. Eight projections, equally spaced over 180 deg, were sequentially recorded. The measurements were performed ~1 mm above the burner head, and the diameter of the aperture was 7 mm. Each pixel corresponds to 120 μm × 120 μm in the flame. The vertical resolution is 370 μm. In order to minimize the effect of small flame fluctuations, each projection measurement was averaged for 10 sec. With the calibration procedure described in the next paragraph the average CH* number density along the rim, i.e., along the intensity maximum of the flame front, was determined to be $\sim 5 \times 10^9$ cm^{-3}.

The detected light power P from the flame is related to the CH* number density n by

$$P = CAh\nu V \frac{\Omega}{4\pi} n, \qquad (1)$$

where C is a system calibration constant, including filter transmission and detector efficiency; A is the Einstein A coefficient [2×10^6 sec^{-1} (Ref. 11)]; h is Planck's constant; ν is the transition frequency; V is the pixel volume; and Ω is the solid angle. We note that, unlike fluorescence measurements of the ground-state number density, measurements of excited-state number density are not affected by quenching, and quantitative results may be obtained. The unknown constants in Eq. (1) were determined by using Rayleigh scattering.[11,17] For these measurements an excimer-pumped dye laser was used to produce 16 mW of vertically polarized light at 431 nm. The flame in Fig. 1 was replaced with a slow flow of nitrogen, and the laser beam was transmitted horizontally through the nitrogen. The scattered light was measured through a polarizer. As the calibration measurements were performed for the same experimental arrangement as the emission measurements, the factors C and Ω in Eq. (1) are determined. However, correction for the polarizer's absorption and the difference in integrated spectral transmission of the interference filter for the broad CH band and the laser light had to be performed.

Simultaneous recording of projections was demonstrated in measurements on a propane–air Bunsen burner. Fluctuations in such a flame result in noisy reconstructions when the projections are sequentially recorded. Figure 1(b) shows the experimental arrangement for the simultaneous recording of three projections. The high spatial resolution of the diode array (25 μm/diode) allows multiple images to be recorded on a single array with sufficient resolution.[18] The long distance (here 1320 mm) between the flame and the lens ensured that the depth of focus for this flame was sufficient for all three projections, although an aperture as large as 36 mm was used. This was verified with the glowing-wire method described above. The two reflected projections were normalized with respect to the center projection to correct for the intensity loss in the mirrors. The setup of Fig. 1(b) can easily be extended to simultaneous measurements of six projections by using two more mirrors, a lens, and another diode-array detector placed on the opposite side of the flame.

Figure 3 shows the CH emission of a slot propane–air Bunsen flame in the top of the premixed inner cone, ~25 mm above the burner. The 41 × 41 pixel picture is reconstructed from three simultaneously recorded projections. Each pixel is 0.53 mm × 0.53 mm, and the vertical resolution is 1.6 mm. The exposure time was 16 msec, and the peak CH* number density is $\sim 1 \times 10^7$ cm^{-3}. This number density is a temporal and spatial average of the fast fluctuations of the

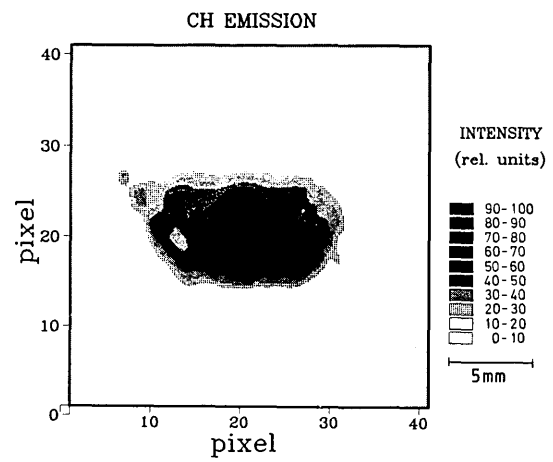

Fig. 3. Tomographic reconstruction of the CH emission of a slot Bunsen flame ~25 mm above the burner. Each pixel is 0.53 mm × 0.53 mm. Three simultaneously recorded projections were used.

flame front. In Fig. 3 broadband soot and chemoluminiscence radiation, which are superimposed upon the CH emission, have been subtracted. Since this background radiation varies slowly with wavelength, the subtraction is easily performed with an additional measurement using the same experimental arrangement with another filter near the CH emission wavelength (here 410 nm). In the methane–oxygen flame this background was negligible.

Reconstruction from few projections requires a tomographic algorithm suited for the specific object to be reconstructed. In this Letter a modified multiplicative algebraic reconstruction algorithm[19] (MART) is used. Simulations show that the modified MART algorithm behaves similarly to the MENT procedure of Minerbo.[20] We have determined that the algorithm behaves well for reconstructions of smooth objects from as few as two or three projections. However, reconstruction of sharp edges, such as those in the methane–oxygen flame, results in strong oscillations on the rim if only two or three projections are used. Simulations show that these oscillations are reduced to a few percent of the average rim value with eight projections. For smoothly varying objects, such as the Bunsen flame, the reconstructions are highly stable even with two or three projections.

Naturally reconstruction from so few projections yields limited spatial resolution. The dependence of the spatial resolution on the number of parallel rays and projection angles is described in Ref. 19. Because of the small number of projection angles used in this study, high-frequency details may be lost, but the overall shape is correctly determined.

The estimated accuracy in the CH* number-density distributions presented in this Letter is ~40%, principally because of errors in the calibration measurement. Other significant errors are reconstruction errors and noise in the reconstructed picture, which together yield a total error of 6–10% of the peak value.

The tomographic algorithm used here assumes negligible self-absorption. From absorption measurements (see, e.g., Ref. 21) it is deduced that the CH self-absorption is negligible in our flames. The same is true for many flame radicals (CH, C_2, CN, etc.) in common flames, although each measurement situation has to be examined individually. An exception is OH, which frequently exhibits strong absorption.

In measurements using the arrangement of Fig. 1(b) care has to be taken to avoid too large a difference in angle between the three beams incident upon the interference filter since this shifts the spectral transmission profile of the filter. In this experiment the difference in angle was ~2 deg, which is negligible.

Because the signal-to-noise ratio in the emission projections is good (~25 for the 16-msec Bunsen measurement), high-temporal-resolution emission tomography is possible. However, it is difficult to give a general estimate of the achievable time resolution since it depends on, e.g., the desired vertical and horizontal resolution, the size of the flame, and the type of fuel–oxidizer. For the propane–air flame we estimate the minimum exposure time required to obtain reliable reconstructions using our experimental geometry to be ~10 msec. While a full image may be acquired in this time, the repetition rate is limited by the optical multichannel analyzer's read-out time of ~17 msec. Owing to the higher number density in the methane–oxygen flame, the minimum exposure time is ~2 orders of magnitude lower in that flame, ~0.1 msec. Tests indicate that exposure times for an acetylene–oxygen flame may be another 1 to 2 orders of magnitude lower. Relaxed requirements on resolution will further decrease the minimum exposure time. Thus time-resolved tomographic imaging of the large-scale development of the flame front in, e.g., explosions or turbulent combustion, should be feasible.

The advice from P.-E. Bengtsson and S. Svanberg is gratefully acknowledged. This project was partially financed by the National Science Foundation, the Carl Trygger Foundation, and the Swedish Board for Technical Development.

References

1. Ed. D. R. Crosley, *Laser Probes for Combustion Chemistry*, ACS Symposium Series (American Chemical Society, Washington, D.C., 1980).
2. Special Issue on Computerized Tomography, Proc. IEEE **71(3)** (1983).
3. H. M. Hertz, Opt. Commun. **54,** 131 (1985).
4. G. W. Faris and R. L. Byer, Opt. Lett. **12,** 155 (1987).
5. W. Alwang, L. Cavanaugh, R. Burr, and A. Hauer, Item 1, Final Rep. PWA-3942 [NAVAIR (Air-602) Contract] (Pratt and Whitney, East Hartford, Conn., 1970).
6. P. J. Emmerman, R. Goulard, R. J. Santoro, and H. G. Semerjian, J. Energy **4,** 70 (1980).
7. T. F. Budinger, G. T. Gullbert, and R. H. Huesman, in *Image Reconstruction from Projections: Implementation and Applications*, G. T. Herman, ed. (Springer-Verlag, New York, 1979), p. 147.
8. R. N. Bracewell, Aust. J. Phys. **9,** 198 (1956).
9. H. N. Olsen, C. D. Maldonado, and G. D. Duckworth, J. Quant. Spectrosc. Rad. Transfer **8,** 1419 (1968).
10. H. Uchiyama, M. Nakajima, and S. Yuta, Appl. Opt. **24,** 4111 (1985).
11. R. G. Joklik, J. W. Daily, and W. J. Pitz, in *Twenty-First Symposium (International) on Combustion* (Combustion Institute, Pittsburgh, Pa., to be published).
12. D. Reuter, B. R. Daniel, J. Jagoda, and B. T. Zinn, Combust. Flame **65,** 281 (1986).
13. S. R. Ray and H. G. Semerjian, in *Digest of Conference on Lasers and Electro-Optics* (Optical Society of America, Washington, D.C., 1985), paper TUB4.
14. R. Snyder and L. Hesselink, Opt. Lett. **13,** 87 (1988); S. Sato, in *Proceedings of International Energy Agency (IEA) 5th Task Leaders Meeting* (IEA, Paris, 1983), p. 157.
15. G. W. Faris and R. L. Byer, "Three-dimensional beam-deflection optical tomography of a supersonic jet," Appl. Opt. (to be published).
16. H. M. Hertz and M. Aldén, Appl. Phys. B **45,** 33 (1988).
17. A. D'Alessio, A. Di Lorenzo, A. Borghese, F. Beretta, and S. Masi, in *Sixteenth Symposium (International) on Combustion* (Combustion Institute, Pittsburgh, Pa., 1976), p. 695.
18. M. Aldén, H. Edner, and S. Svanberg, Appl. Phys. B **29,** 93 (1982).
19. H. M. Hertz, Appl. Opt. **25,** 914 (1986).
20. G. Minerbo, Comput. Graph. Image Process. **10,** 48 (1979).
21. R. Bleekrode and W. C. Nieuwpoort, J. Chem. Phys. **43,** 3680 (1965).